Available online at www.sciencedirect.com
ScienceDirect
International Journal of Heat and Mass Transfer 51 (2008) 1713–1727
International Journal of HEAT and MASS TRANSFER
www.elsevier.com/locate/ijhmt

# Notable physical anomalies manifested in non-Fourier heat conduction under the dual-phase-lag model

B. Shen, P. Zhang *

*Institute of Refrigeration and Cryogenics, Shanghai Jiao Tong University, Shanghai 200240, China*

Received 17 November 2006; received in revised form 14 April 2007
Available online 20 September 2007

**Abstract**

In this study, a number of notable physical anomalies concerning non-Fourier heat conduction under the dual-phase-lag (DPL) model are observed and investigated. It is found that, during the transient heat transfer process, the over-diffusion mode predicts a "hyper-active" to "under-active" transition in thermal behavior. The main cause behind it lies in the time-varying effect of $\tau_T$ (the phase lag of the temperature gradient) on the thermal response. Also, change of polarity in reflected thermal waves can be observed when a constant-temperature boundary is involved, which hints that a heating process may be followed by a spontaneous cooling effect. A fairly strong connection is present between the $\tau_T$-induced dispersive effect and an unusual thermal accumulation phenomenon in an on–off periodic heating process. Furthermore, a paradox involving a moving medium is detected in the DPL model, which can be solved by replacing the temporal partial derivatives in the DPL equation with the material derivatives. During the process of analysis, a high-order characteristics-based TVD scheme is relied on to provide accurate and reliable numerical simulations to the DPL heat conduction equation under various initial-boundary conditions.


*Keywords:* Non-Fourier heat conduction; Dual-phase-lag model; Total-variation-diminishing scheme; Physical anomalies

## 1. Introduction

After witnessing a myriad of substantive and comprehensive breakthroughs in the science of heat transfer in the past century or so, Fourier's law of heat conduction remains as one of the few empirical theories that are solely based on experimental observations and, at the same time, enjoying a large variety of applications in daily engineering practice nevertheless. Despite the fact that, Fourier's law implies that thermal signal travels at an infinite velocity when combined with energy conservation equation, it is fair to say that the classical heat conduction model yields excellent descriptions of various thermal transportation behaviors in a single-phase medium under most circumstances. However, when it comes to high-rate heating process (duration time on the order of femtoseconds) [1] or helium cryogenic engineering (near absolute zero) [2], the wave nature of heat conduction which is displayed in these situations, such as sharp wave front and finite velocity of thermal propagation, dismisses Fourier's law completely incapable—if not useless—to provide reasonable and decent predictions that capture these non-Fourier effects.

To alleviate this physically unrealistic notion of instantaneous energy diffusion, Cattaneo [3] and Vernotte [4] postulated a modified Fourier's law, commonly known as the thermal wave model, which in essence hypothesizes that there exists a time delay between the temperature gradient imposed and the heat flux to generate. This newly-developed hyperbolic heat conduction model, to some extent, fills the holes in the theoretical foundation of the classical diffusion theory and shows a great amount of promise of superseding it when extreme situations are involved (ultra-short period of time, small domain, exceedingly sharp temperature gradient or very low temperature) [5–9]. However, discernible discrepancies between theoretical predictions

* Corresponding author. Tel.: +86 21 34205505; fax: +86 21 34206814.
*E-mail address:* zhangp@sjtu.edu.cn (P. Zhang).

0017-9310/$ - see front matter © 2007 Elsevier Ltd. All rights reserved.
doi:10.1016/j.ijheatmasstransfer.2007.07.039

**Nomenclature**

| | |
|---|---|
| $c_p$ | specific heat capacity at constant pressure |
| **E** | vector defined in Eq. (10) |
| **F** | vector defined in Eq. (10) |
| **G** | vector defined in Eqs. (12c) and (44) |
| $k$ | thermal conductivity |
| $L$ | characteristic length |
| $n$ | number of period in Eq. (25) |
| $P$ | duration of period in Eq. (25) |
| $q$ | heat flux |
| **q** | heat flux vector |
| $Q$ | dimensionless heat flux |
| **r** | spatial vector |
| **S** | vector defined in Eq. (10) |
| $t$ | time variable |
| $T$ | temperature |
| $T_r$ | reference temperature |
| $u$ | velocity |
| **u** | velocity vector |
| $U$ | dimensionless temperature |
| **v** | relative velocity vector of a moving frame to a medium in motion |
| **V** | velocity vector of a moving frame |
| **W** | vector defined in Eqs. (12a) and (42) |
| $x$ | spatial variable |
| $Z$ | dimensionless phase lag |

*Greek symbols*

| | |
|---|---|
| $\alpha$ | thermal diffusivity |
| $\beta$ | dimensionless time |
| $\theta$ | dimensionless temperature in a moving frame |
| $\Lambda$ | dimensionless velocity of a moving medium |
| $\lambda_j$ | eigenvalue, $j = 1, 2$ |
| $\xi$ | dimensionless spatial variable |
| $P$ | density in a moving frame |
| $\rho$ | density |
| $\tau$ | phase lag |
| $\chi$ | dimensionless spatial variable in a moving frame |
| $\boldsymbol{\chi}$ | spatial vector in a moving frame |
| $\Psi$ | dimensionless heat flux in a moving frame |
| $\boldsymbol{\Psi}$ | heat flux vector in a moving frame |
| $\Omega$ | temperature in a moving frame |

*Subscripts*

| | |
|---|---|
| $q$ | heat flux |
| $T$ | temperature gradient |

and experimental results [10], along with lacking in firm physical basis to support [11], leave the validity of the thermal wave model open to debate. As opposed to the "crisis" encountered in the application of the hyperbolic heat conduction model, the two-step model pioneered by Anisimov et al. [12] and the pure phonon field in dielectric crystals successfully obtained by Guyer and Krumhansl [13] helped shed light on the mechanism of the non-equilibrium thermodynamic transition and the energy exchange on the microscopic level. To incorporate these microscopic effects into a macroscopic description (that most practicing engineers are more acquainted with), Tzou [14] proposed the widely-celebrated dual-phase-lag (DPL) model. This universal model is claimed to be able to smoothly bridge the gap between the microscopic and the macroscopic approach, covering a wide range of heat transfer models (reducing to the classical diffusion model, the controversial thermal wave model, the two-step phonon–electron interaction model for metals, and the pure phonon scattering model for insulators, semiconductors and dielectric films, simply by adjusting the value of $\tau_q$ and $\tau_T$, the two primary time relaxation parameters in the governing equation).

Recently the DPL heat conduction model has stimulated considerable interest in the heat transfer community, by offering alternative interpretations and new perspectives to a large body of non-Fourier thermal behaviors in energy transportation process under special considerations, such as heat conduction in biological materials [15], heat transport in amorphous media [16] and layered-film heating in superconductors, fins and reactor walls [17]. Needless to say, numerous efforts have been invested to the development of an explicit mathematical solution to the heat conduction equation under the DPL model: Tzou et al. [18] solved the one-dimensional initial-boundary value problem with a surface temperature-jump disturbance through numerically computing the inverse Laplace transformation integral with Riemann sum approximation. Antaki [19] derived a solution for transient temperature in a semi-infinite slab subjected to a constant surface heat flux by first using the Fourier sine transformation to eliminate the space-derivatives and then taking the Laplace transformation to remove the time-derivatives in the heat conduction equation. Tang and Araki [20] obtained the temperature distribution in a finite slab with an energy source near the surface using Green's function method and finite integral transformation technique. Liu [17] relied on a hybrid application of the Laplace transformation method and a control-volume formulation to analyze the DPL effect on the heating in two-layered thin films with an interfacial thermal resistance. Most of these analytical solutions to the DPL heat conduction problems in the literature were formulated ad hoc, only applicable to specific formulations of initial-boundary conditions. Other than the notoriously annoying fictitious numerical oscillations frequently encountered in solving hyperbolic partial differential equations (HPDE), the intrinsic complexity of the DPL heat conduction equation alone (high-order mixed derivative with respect to space and time) poses a tremendous hinder-

ing obstacle against a general solution. Whenever a complicated geometry or a variable physical property is involved, numerical solution is always considered the best (and maybe the only) option.

The present work employs a purely numerical explicit TVD (total-variation-diminishing) scheme—which is formulated based on the method proposed by Yang [21] in his investigation of the thermal wave equation—to solve the DPL heat conduction equation under various initial-boundary conditions. Calculations are performed to exhibit a number of the physical irregularities concerning the DPL thermal behavior that the classical diffusion theory or the thermal wave model fails to capture. In-depth analyses are included accordingly to offer possible mathematical or physical interpretation to these anomalies.

## 2. Mathematical formulation

Fourier's law of heat conduction states that the heat flux is directly proportional to the temperature gradient at any time and at any point in the medium:

$$\mathbf{q}(\mathbf{r},t) = -k\nabla T(\mathbf{r},t) \tag{1}$$

To account for the micro-scale effect such as the phonon–electron interaction, the DPL model introduces two phase lags, also known as the relaxation times, to both the heat flux and the temperature gradient. The corresponding macro-scale lagging behavior is thus described as

$$\mathbf{q}(\mathbf{r},t+\tau_q) = -k\nabla T(\mathbf{r},t+\tau_T) \tag{2}$$

This constitutive equation dictates that the temperature gradient established at a position $\mathbf{r}$ at time instant $t+\tau_T$ causes the heat to flow at a different instant of time $t+\tau_q$. Mathematically speaking, the heat flux precedes the temperature gradient for $\tau_q < \tau_T$, whereas the temperature gradient precedes the heat flux for $\tau_q > \tau_T$. From a physical point of view though, the case $\tau_q < \tau_T$ is suspected to lead to some unacceptable conclusions, which is one of the major theoretical controversies hovering over the validity of the DPL model. As Zhou et al. [22] strongly criticized, the DPL model might violate the second law of thermodynamics when $\tau_q < \tau_T$, implying that heat flows from a low-temperature region to a high-temperature region spontaneously. Such a seemingly non-physical notion, however, can be well explained and corroborated by the non-equilibrium entropy production theory [23]. Moreover, a large part of the applications of the DPL model are, as a matter of fact, specifically related to the case $\tau_q < \tau_T$, such as the ultrafast pulse-laser heating on metal films [24]. Therefore, we allow the case of $\tau_T$ being greater than $\tau_q$ in part of this investigation, although the majority of our concentration still focuses on the unique features of the DPL model under the condition $\tau_q > \tau_T$.

The phase lags $\tau_q$ and $\tau_T$ are both positive-valued intrinsic properties of the material in question (for instance, $\tau_q = 0.1670$ ps and $\tau_T = 12.097$ ps for Pb [14], whereas $\tau_q$ is estimated to be 61.18 ps and $\tau_T$ less than 0.005 ps for solid $He^4$ [20]). Taking a first-order Taylor series expansion on the both sides of Eq. (2) with reference to t yields

$$\mathbf{q}(\mathbf{r},t) + \tau_q \frac{\partial \mathbf{q}}{\partial t}(\mathbf{r},t) = -k\left\{\nabla T(\mathbf{r},t) + \tau_T \frac{\partial}{\partial t}[\nabla T(\mathbf{r},t)]\right\} \tag{3}$$

Combining Eq. (3) and the energy conservation equation with constant thermal properties and no heat source, given as below

$$\rho c_p \frac{\partial T}{\partial t}(\mathbf{r},t) + \nabla\cdot\mathbf{q}(\mathbf{r},t) = 0 \tag{4}$$

results in the $T$ representation of the DPL heat conduction equation

$$\nabla^2 T + \tau_T \frac{\partial}{\partial t}(\nabla^2 T) = \frac{1}{\alpha}\frac{\partial T}{\partial t} + \frac{\tau_q}{\alpha}\frac{\partial^2 T}{\partial t^2} \tag{5}$$

where $\alpha = k/(\rho c_p)$ is the thermal diffusivity. Eq. (5) is a rather complicated partial differential equation which illustrates various physical characteristics depending on the selection of $\tau_q$ and $\tau_T$. By comparing with the classical diffusion equation ($\tau_q = \tau_T = 0$), it is evident that the phase lag of the heat flux $\tau_q$ is responsible for the wave nature of non-Fourier heat conduction. On the other hand, the phase lag of the temperature gradient $\tau_T$ brings an additional diffusion-like feature into the thermal wave equation ($\tau_T = 0$ and $\tau_q \neq 0$).

For one-dimensional problems, Eqs. (3) and (4) takes the form as

$$q(x,t) + \tau_q \frac{\partial q}{\partial t}(x,t) = -k\frac{\partial T}{\partial x}(x,t) - k\tau_T \frac{\partial^2 T}{\partial t \partial x}(x,t) \tag{6}$$

$$\rho c_p \frac{\partial T}{\partial t}(x,t) + \frac{\partial q}{\partial x}(x,t) = 0 \tag{7}$$

By introducing the following dimensionless quantities:

$$\xi = x/L \tag{8a}$$

$$\beta = t\alpha/L^2 \tag{8b}$$

$$U = (T - T_r)/T_r \tag{8c}$$

$$Q = qL/kT_r \tag{8d}$$

$$Z_q = \tau_q\alpha/L^2 \tag{8e}$$

$$Z_T = \tau_T\alpha/L^2 \tag{8f}$$

Eqs. (6) and (7) can be rewritten in the dimensionless vector form as

$$\frac{\partial \mathbf{E}}{\partial \beta} + \frac{\partial \mathbf{F}}{\partial \xi} = \mathbf{S} \tag{9}$$

where

$$\mathbf{E} = \begin{bmatrix} Z_q Q \\ U \end{bmatrix}, \quad \mathbf{F} = \begin{bmatrix} U \\ Q \end{bmatrix}, \quad \mathbf{S} = \begin{bmatrix} -Q - Z_T \frac{\partial^2 U}{\partial \xi \partial \beta} \\ 0 \end{bmatrix} \tag{10}$$

Following the steps of diagonalization based on eigenvalues described thoroughly in [21], we can reformulate

the above vector equation into two separately independent equations

$$\frac{\partial W_j}{\partial \beta} + \lambda_j \frac{\partial W_j}{\partial \xi} = G_j, \quad j = 1, 2 \tag{11}$$

with the new variables defined as

$$\begin{bmatrix} W_1 \\ W_2 \end{bmatrix} = \begin{bmatrix} \frac{1}{2}\left(\sqrt{Z_q}Q + U\right) \\ \frac{1}{2}\left(U - \sqrt{Z_q}Q\right) \end{bmatrix} \tag{12a}$$

$$\begin{bmatrix} \lambda_1 \\ \lambda_2 \end{bmatrix} = \begin{bmatrix} 1/\sqrt{Z_q} \\ -1/\sqrt{Z_q} \end{bmatrix} \tag{12b}$$

$$\begin{bmatrix} G_1 \\ G_2 \end{bmatrix} = \begin{bmatrix} \frac{-1}{2\sqrt{Z_q}}\left(Q + Z_T \frac{\partial^2 U}{\partial \beta \partial \xi}\right) \\ \frac{1}{2\sqrt{Z_q}}\left(Q + Z_T \frac{\partial^2 U}{\partial \beta \partial \xi}\right) \end{bmatrix} \tag{12c}$$

The above equations can be readily solved by the high-order TVD scheme with Roe's superbee limiter function, the detail of which can be found in [21].

## 3. Validation of the numerical method

Before presenting the uncommon phenomena observed in the heat transfer process in the framework of the DPL model, we need to test the validity of this adopted TVD scheme in solving the DPL equation. The basic idea of the TVD scheme is to combine the low-order and high-order finite-difference schemes. It guarantees second-order accuracy in the smooth part of the solution where the temperature variation is relatively gradual, and automatically switches to the first-order scheme whenever sharp discontinuities are involved, thus avoiding spurious numerical oscillations. Traditionally employed for the numerical investigation of the well-known thermal wave heat conduction equation ($\tau_T = 0$), the present numerical scheme is reported to be effective and reliable in capturing non-Fourier features [21,25]. Yet its applicability in solving the DPL model has not been justified. A comparison between the numerical solution employing the TVD scheme and the analytical solution available in the literature regarding the same one-dimensional heat conduction problem ($0 \leqslant \xi \leqslant 1$, $\beta > 0$) is conducted. The initial-boundary conditions are given as follows

$$U = 0 \quad \text{and} \quad \frac{\partial U}{\partial \beta} = 0 \quad \text{at } \beta = 0 \tag{13}$$

$$U = 1 \quad \text{at } \xi = 0 \tag{14}$$

$$Q = 0 \quad \text{at } \xi = 1 \tag{15}$$

The results are plotted in Fig. 1. It is fairly obvious that the present numerical predictions of the spatial temperature distributions with a wide range of $Z_T$ variation (from 0 to 0.5) at the instant $\beta = 0.05$ are in perfect agreement with those obtained by Tzou [14], which justifies the credibility and reliability of the TVD scheme in solving the DPL heat conduction equation.

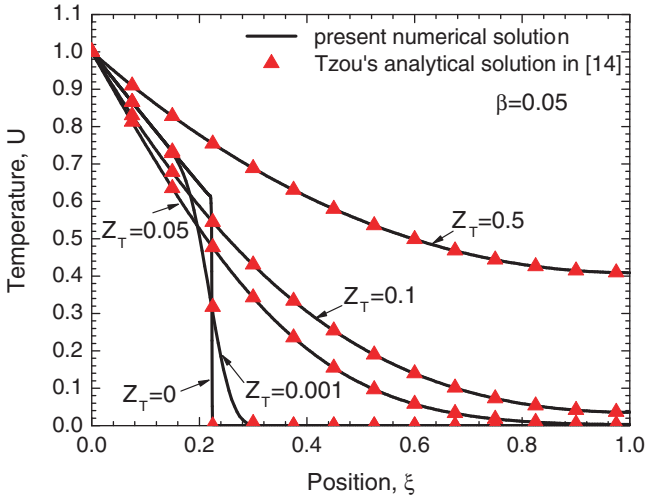


Fig. 1. Comparison between the spatial temperature distributions obtained by the present numerical method and the analytical solution regarding the 1-D problem with initial-boundary conditions defined in Eqs. (13)–(15) at $\beta = 0.05$ for $Z_q = 0.05$ and various $Z_T$ values.

Additionally, distinct transitions with increasing $Z_T$ in transient thermal response can be clearly observed in Fig. 1, from wave ($Z_T = 0$) to wavelike ($0 < Z_T < Z_q$) to diffusion ($Z_T = Z_q$, since no phase lag exists between the temperature gradient and the heat flux, which according to [14] is the more general condition for reduction to diffusion in absence of an initial temperature rate) to over-diffusion ($Z_T > Z_q$), in accordance with Tang and Araki's classification [20]. When $Z_T = 0$, the temperature curve corresponds with the prediction of the classical thermal wave model. As shown in Fig. 1, a sharp temperature jump defines the thermal wave front, beyond which the temperature remains undisturbed. As $Z_T$ increases, the effect of $\tau_T$ starts to influence the heat conduction process, smoothing the temperature wave front and stretching the thermal-affected region deeper into the medium. Strictly speaking, there is no thermal waves present at this time, because the corresponding DPL equation (Eq. (5)) is essentially parabolic just like the pure diffusion equation and consequently suffers from the same conceptual pitfall, which is energy travels at an infinite velocity. Nevertheless, in a broader sense, we still refer to this particular kind of temperature distribution as thermal waves, as long as $Z_T < Z_q$ (when the wave features are yet observable in the heat transfer process). Once $Z_T$ exceeds $Z_q$, all wave features of heat conduction disappear, and a diffusion-like thermal behavior—which noticeably deviates from the classical diffusion theory's prediction (see Fig. 1)—becomes dominant. This phenomenon will be discussed at length in the next section.

## 4. Results and discussion

### 4.1. Diffusion versus over-diffusion

As Fig. 1 shows, the temperature level of over-diffusion ($Z_T > Z_q$) exceeds that of diffusion ($Z_T = Z_q$) at $\beta = 0.05$.

In other words, it seems that positive difference between $Z_T$ and $Z_q$ results in an exceptionally rapid thermal response to the change of left-end boundary condition ($U=1$ at $\xi=0$) at early time. As time elapses, however, the temperature under the diffusion mode eventually "overtakes" that under the over-diffusion mode at $\beta=1$ in achieving the ultimate thermal equilibrium state, which happens to be unity of temperature at every point in the medium in this case (see Fig. 2). As far as temperature level goes, the term "over-diffusion" turns out to be somewhat a misnomer for the case $Z_T > Z_q$ since the highly sensitive thermal behavior only last for a short period of time. Its promoting effect on the heat transfer is well offset by the thermal "inertness" manifested at a later stage. This odd "hyper-active" to "under-active" thermal behavior in connection with the so-called over-diffusion has been reported by Tzou [14] and Tang et al. [20]. But neither gives any convincing explanation regarding its underlying causes. We now attempt an interpretation to this phenomenon from a mathematical point of view.

Inspired by Kulish and Novozhilov's elegant treatment to the DPL equation [26], instead of the approximation form, we start the process of analysis with the general form of the constitutive DPL relation, Eq. (2). With the one-dimensional configuration, the constitutive equation becomes

$$q(x,t+\tau_q) = -k\frac{\partial T}{\partial x}(x,t+\tau_T) \tag{16}$$

Since $\tau_T$ is larger than $\tau_q$ in the over-diffusion mode, Eq. (16) can also be written as

$$q(x,t+\tau_T) = -k\frac{\partial T}{\partial x}[x,t+\tau_T+(\tau_T-\tau_q)] \tag{17}$$

With the observation time shifting from $t$ to $t+\tau_T$, the energy conservation equation is given as

$$\rho c_p\frac{\partial T}{\partial t}(x,t+\tau_T) + \frac{\partial q}{\partial x}(x,t+\tau_T) = 0 \tag{18}$$

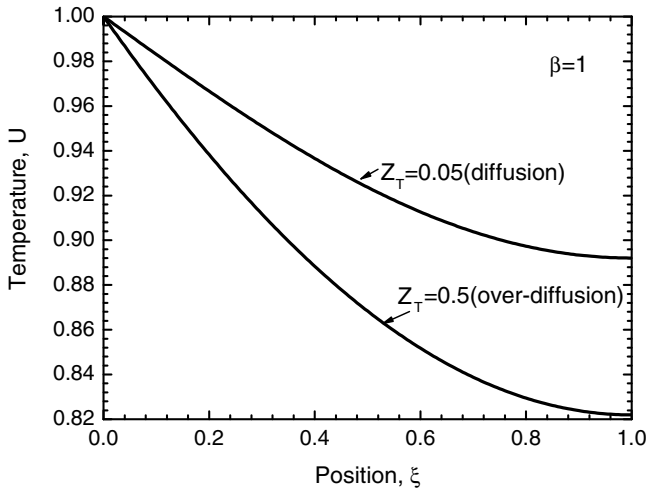


Fig. 2. Spatial temperature distributions regarding the 1-D problem with initial-boundary conditions defined in Eqs. (13)–(15) at $\beta=1$ for $Z_q=0.05$ and various $Z_T$ values.

Substituting Eq. (17) into Eq. (18) and eliminating the heat flux $q$ yields

$$\rho c_p\frac{\partial T}{\partial t}(x,t+\tau_T) = k\frac{\partial^2 T}{\partial x^2}[x,t+\tau_T+(\tau_T-\tau_q)] \tag{19}$$

With the new time variable defined as $t^*=t+\tau_T$, expanding the above equation with reference to $t^*$ leads to

$$\rho c_p\frac{\partial T}{\partial t}(x,t^*) = k\left\{\frac{\partial^2 T}{\partial x^2}(x,t^*) + (\tau_T-\tau_q)\frac{\partial}{\partial t}\left[\frac{\partial^2 T}{\partial x^2}(x,t^*)\right]\right\} \tag{20}$$

Compared with the classical diffusion equation with observation time $t^*$

$$\rho c_p\frac{\partial T}{\partial t}(x,t^*) = k\frac{\partial^2 T}{\partial x^2}(x,t^*) \tag{21}$$

it has been made clear that the primary difference between the DPL conduction and the classical thermal diffusion lies in the extra term on the right side of Eq. (20), which is factored by $(\tau_T-\tau_q)$. When $\tau_T$ equals $\tau_q$, the DPL equation reduces to the identical form to the diffusion equation, which is consistent with Tzou's notion [14] that without any heat source, the more general condition for the reduction of the DPL model to diffusion should be taken as $\tau_T=\tau_q$.

As a result of the current set of the initial-boundary conditions in question (the left-end temperature experiencing a sudden step change while the right-end boundary kept insulated), no energy loss is expected to occur at both boundary surfaces. Guaranteed continuous increase of temperature in the medium results in the downward convex-shape of the spatial temperature distribution curves (since the second-order spatial derivative of temperature assumes positive value, see Eqs. (20) and (21)). At the early stage of the heat conduction, the temperature distribution in the medium, in response to a sudden temperature rise at the left-end boundary ($U=1$ at $\xi=0$), evolves from the initial isothermal state (or an horizontal straight line, $U=0$ at $\beta=0$) to the crescent shape which is consistent with the positive second-order spatial derivative. Hence, the time rate of change of the second-order spatial derivative of temperature most certainly assumes positive value. Given the fact that $\tau_T$ is larger than $\tau_q$ for over-diffusion, the extra term on the right-side of Eq. (20) thus contributes as "a thrusting force" to the heating process in the medium (increasing the time rate of temperature rise). On the other hand, as the medium temperature approaches its ultimate thermal equilibrium ($U=1$), the temperature curve is once again reaching a uniformity similar to the initial state. Due to the process of reversing, the time rate of change of the second-order spatial derivative of temperature must assume negative value instead. This time the extra term acts as "a dragging force" to the so called over-diffusive heat conduction (practically slowing down the process of temperature rise). Fig. 3 displays the variation of the second-order spatial derivative of temperature versus time at the

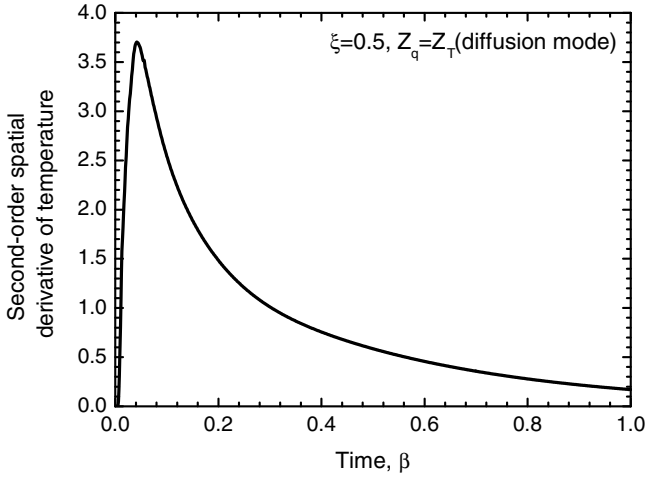


Fig. 3. Second-order spatial derivative of temperature versus time regarding the 1-D problem under the diffusion mode ($Z_q = Z_T$) with initial-boundary conditions defined in Eqs. (13)–(15) at $\xi = 0.5$.

midpoint of the medium ($\xi = 0.5$) under the diffusion mode ($Z_T = Z_q$). It explicitly shows that the second-order spatial derivative experiences a slope change from positive to negative, which is consistent with our previous discussion. In Fig. 4, it shows the time-history of the local temperature evolution at $\xi = 0.5$. It is obvious that the course of temperature rise goes through a phase of gradual "slowing-down" after a brief but significant "spike".

### 4.2. Inverted-reflection phenomenon

The phenomenon of reflection is one of the most fascinating features of the classical thermal wave propagation. Especially for thermal processing of layered media, the transmission–reflection phenomenon between dissimilar materials has drawn a fair amount of attention [17,27]. Since the classical thermal wave hypothesis is a special case of the DPL model ($\tau_T = 0$), certainly the wave reflection phenomenon merits a place in our investigation of the DPL heat conduction under the generalized wave mode ($\tau_T < \tau_q$).

Consider a one-dimensional slab with the same initial thermal condition as defined in Eq. (13). At $\beta = 0$, a short-duration heat pulse enters the medium from the left-end boundary

$$Q = 2 \quad \text{at } \xi = 0, \quad 0 < \beta < 0.05 \tag{22}$$

At the right-end boundary, two different boundary conditions are given as

$$U = 0 \quad \text{at } \xi = 1 \quad \text{(zero temperature)} \tag{23}$$

and

$$Q = 0 \quad \text{at } \xi = 1 \quad \text{(zero heat-flux)} \tag{24}$$

It should be noted that the zero-temperature condition here essentially indicates constant temperature at the right boundary since $U$ is directly proportional to the difference between the medium temperature and the reference temperature. Figs. 5 and 6 demonstrate the spatial temperature distributions of the incoming thermal waves and the reflected waves with the zero-temperature and the zero-heat-flux right-end boundary conditions, respectively. Surprisingly, two distinct patterns of reflection are observed: Regardless of $Z_T$, whereas positive reflected thermal waves are bounced off the adiabatic boundary (the zero-heat-flux boundary) as expected (see Fig. 6), the zero-temperature boundary produces "inverted" temperature wave fronts of the reflected thermal waves (which in essence means that the reflected thermal waves assume temperature of the opposite polarity to the incoming ones as though they were turned upside down, as shown in Fig. 5). As odd as it sounds, this notion implies that, if the temperature of the

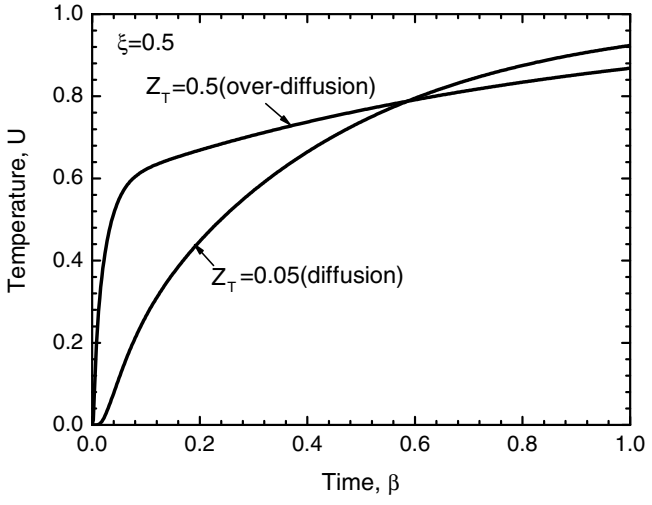


Fig. 4. Temperature versus time regarding the 1-D problem at $\xi = 0.5$ for $Z_q = 0.05$ and various $Z_T$ values with initial-boundary conditions defined in Eqs. (13)–(15).

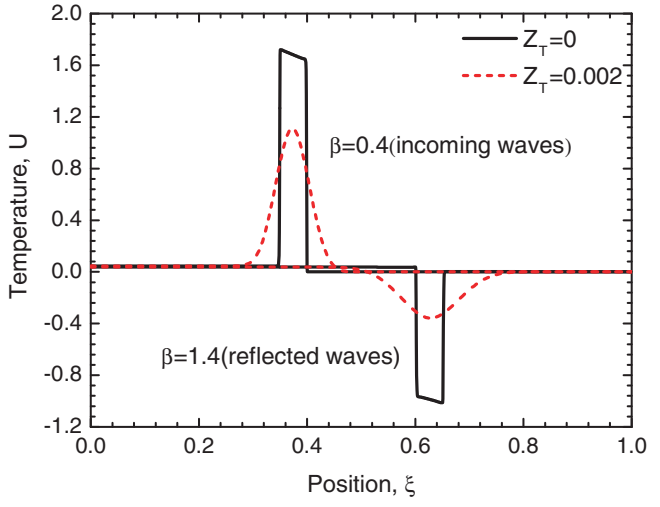


Fig. 5. Spatial temperature distributions in a finite slab with initial condition defined in Eq. (13), left-end boundary condition defined in Eq. (22) and zero-temperature right-end boundary condition for $Z_q = 1$ and (—) $Z_T = 0$; (--) $Z_T = 0.002$.

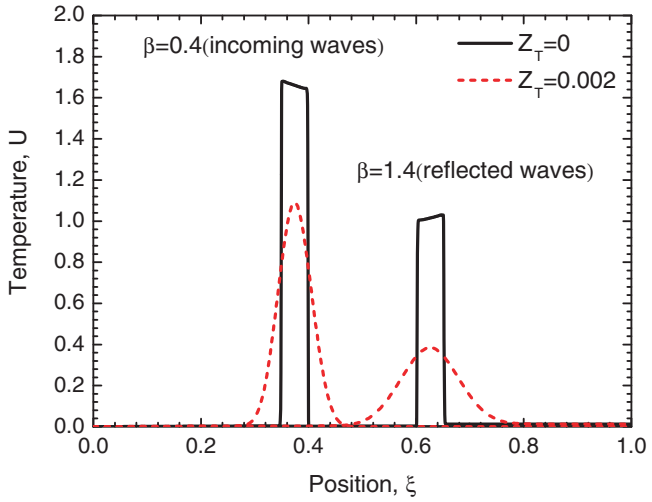


Fig. 6. Spatial temperature distributions in a finite slab with initial condition defined in Eq. (13), left-end boundary condition defined in Eq. (22) and zero-heat-flux right-end boundary condition for $Z_q = 1$ and (—) $Z_T = 0$; (--) $Z_T = 0.002$.

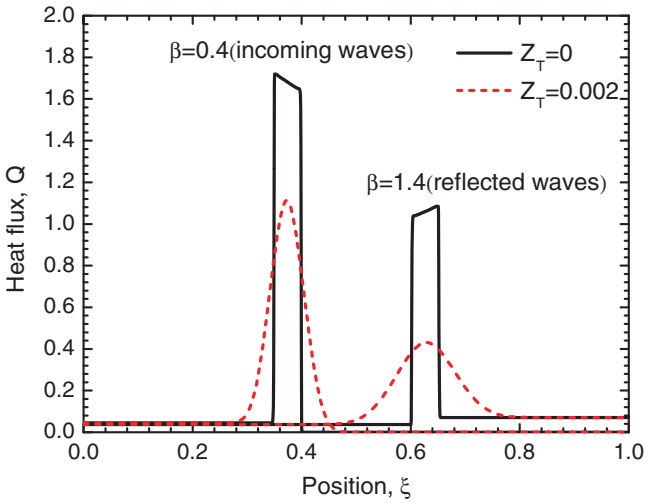


Fig. 7. Spatial heat flux distributions in a finite slab with initial condition defined in Eq. (13), left-end boundary condition defined in Eq. (22) and zero-temperature right-end boundary condition for $Z_q = 1$ and (—) $Z_T = 0$; (--) $Z_T = 0.002$.

other end is maintained constant, the heating process in a finite medium, a one-dimensional slab for example, might as well end up cooling instead! In theory, one of the physical applications of this unusual feature is that the generalized cooling effects could be achieved without resorting to a heat source of lower temperature. It is worth noting that such singularity should not be confused with the anomalous results reported by Haji-Sheikh et al. [28] regarding the interaction of a thermal wave front and a boundary. As demonstrated in detail in [28], a sharp wave front arriving at an insulated boundary may lead to physically unacceptable results such as a temperature drop due to heating, which is believed to be an intrinsic mathematical flaw in analytical solutions to the thermal wave propagation in general. In our investigation, however, the inverted-reflection phenomenon in question, as will be analyzed and discussed below, is an inherent physical characteristic of the DPL thermal behavior instead.

In contrast, the spatial distributions of the heat fluxes with the same conditions are displayed in Figs. 7 and 8. The exactly opposite conclusion can be drawn: The reflected thermal waves assume positive heat flux value in the case of the zero-temperature boundary (see Fig. 7), while negative heat fluxes appear when the boundary is assumed to be adiabatic (see Fig. 8).

A simple and illustrative analogy can be drawn between thermal waves and mechanical waves regarding the reflection phenomenon. Likewise, there exist two dissimilar boundary conditions for mechanical waves also: fixed-end and free-end. At the fixed-end boundary, the local displacement is supposed to be zero. As can be seen in Fig. 9a and c, the reflected waves take on two different kinds of wave shape. To be specific, the reflected wave for displacement appears to be the "inverted" image of the incoming wave (see Fig. 9a), while the reflected wave for stress remains in every aspect symmetrical to the incoming one (see

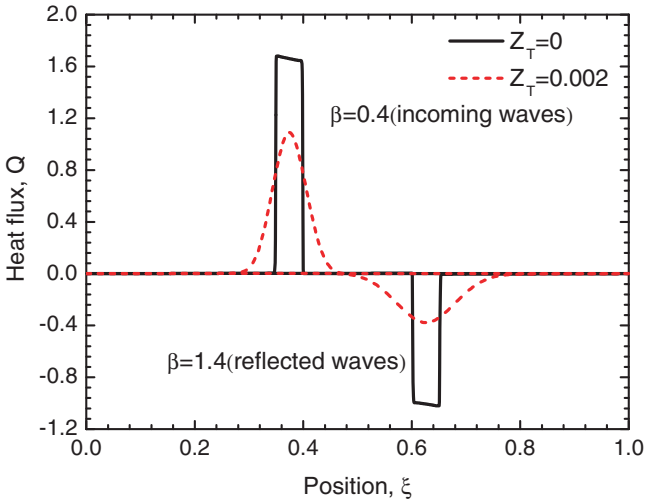


Fig. 8. Spatial heat flux distributions in a finite slab with initial condition defined in Eq. (13), left-end boundary condition defined in Eq. (22) and zero-heat-flux right-end boundary condition for $Z_q = 1$ and (—) $Z_T = 0$; (--) $Z_T = 0.002$.

Fig. 9c). To help understand this singularity intuitively, one needs to imagine the reflected wave propagates toward the boundary from outside of the medium, making contact with the incoming wave at the boundary. As the fixed-end boundary is applied, the reflected wave front ought to assume the same amplitude of displacement from the equilibrium position as the incoming one except with an opposite sign, so as to cancel each other out at the boundary to comply with the strict zero-displacement requirement. As a result, the reflected displacement wave and the incoming wave, in essence, make up a pair of "inverted" mirror image as displayed in Fig. 9a. It is noted that because the stress is directly proportional to the first-order spatial derivative of the displacement for mechanical waves, the

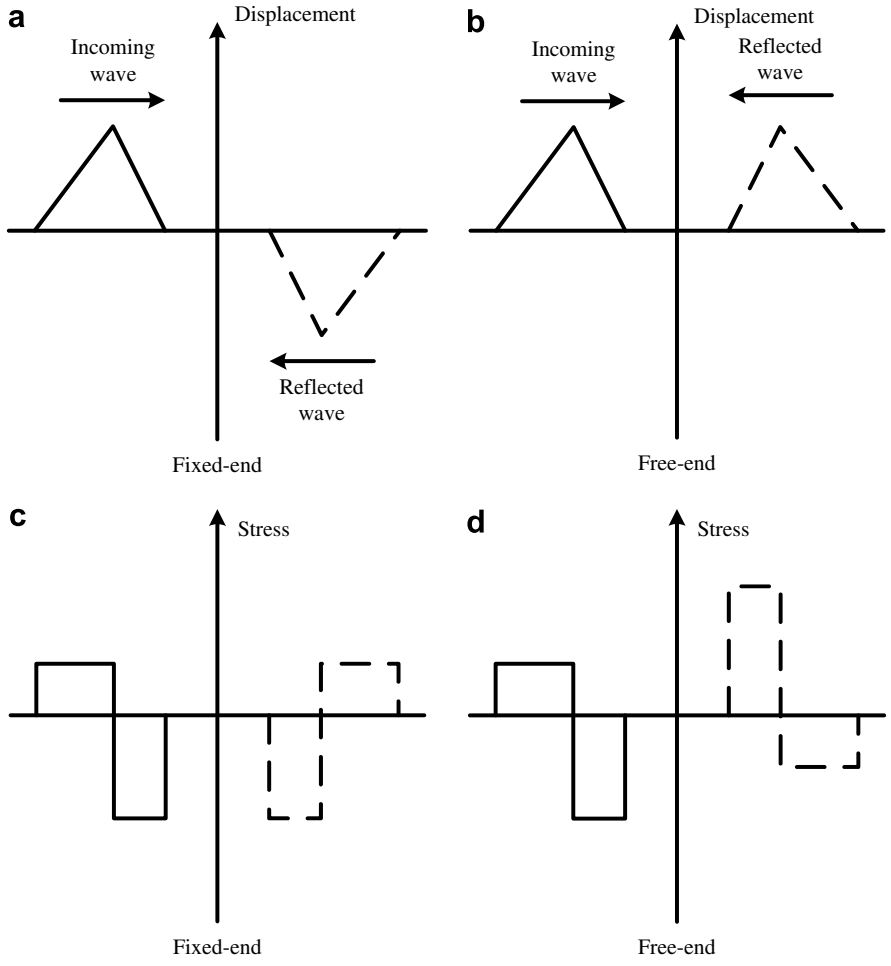


Fig. 9. Analogy with mechanical wave motion concerning reflected waves of, (a) displacement from a fixed-end boundary; (b) displacement from a free-end boundary; (c) stress from a fixed-end boundary; (d) stress from a free-end boundary.

reflected wave for stress assumes the same polarity and shape as the incoming wave (see Fig. 9c). As for the case of thermal waves, the same line of logic can be readily applied for the zero-temperature boundary. Since no temperature disturbance is allowed at the zero-temperature boundary, the reflected temperature wave has to assume negative value as opposed to the incoming wave, as illustrated in Fig. 5.

On the other hand, whenever the free-end boundary is involved, it is the stress that is demanded to be zero at the boundary, which leads to the "inverted" wave shape of the reflected stress wave, as shown in Fig. 9d. Once again due to the mathematical relation between the displacement and the stress as mentioned above, consequently it is the reflected displacement wave that assumes the exact shape of "mirror" image of the incoming wave (see Fig. 9b). Similarly, one can draw an analogous argument regarding the thermal wave reflection at the zero-heat-flux boundary. When the adiabatic boundary is imposed, the heat flux—rather than the temperature—of the reflected wave should assume the opposite polarity (see Fig. 8). The comparison between thermal waves and mechanical waves is summarized in Table 1.

It is quite interesting to note that when the zero-temperature boundary is applied, the heat fluxes for both the incoming thermal waves and the reflected waves are positive even though the energy transfer obviously alters its direction after the reflection incident from the boundary, as shown in Fig. 7. Unlike under the classical diffusion model, there seems to be no direct correlation between the sign of heat flux and the direction of energy transportation in a one-dimensional DPL heat conduction process, especially for a short-duration pulse-shaped surface thermal disturbance as is in this case study. In other words, the reflected thermal waves under such conditions do not necessarily assume negative heat flux values.

In the classical diffusion theory, the straightforward and direct mathematical relation between the heat flux and the temperature gradient (see Eq. (1)) not only results in smooth and continuous distributions of temperature in space, but also produces a rather simple connection between the sign of heat flux and the direction of energy transmission. Positive heat flux leads to negative temperature gradient, which according to the thermodynamics second law causes energy to flow in the positive spatial direction (high temperature to low temperature).

Table 1
Summary of analogy between the reflection phenomenon of thermal waves and mechanical waves

| | Thermal waves | Mechanical waves |
|---|---|---|
| *Mathematical aspect* | | |
| Governing equation[a] | $(1/\alpha)\partial T/\partial t + (\tau_q/\alpha)\partial^2 T/\partial t^2 = \partial^2 T/\partial x^2 + \tau_T \partial(\partial^2 T/\partial x^2)/\partial t$ | $\partial^2 u/\partial t^2 = c^2 \partial^2 u/\partial x^2$ [b] |
| Variables | Temperature, $T$<br>Heat flux, $q$ | Displacement, $u$<br>Stress, $F$[c] |
| *Physical aspect* | | |
| Reflection pattern at the boundary | Change of wave polarity for temperature at the zero-temperature boundary<br>Change of wave polarity for heat flux at the adiabatic boundary | Change of wave polarity for displacement at the fixed-end boundary<br>Change of wave polarity for stress at the free-end boundary |

[a] Only one-dimensional form is given.
[b] $u$ is the longitudinal displacement, and parameter c is the wave speed.
[c] Stress $F$ is directly proportional to the first-order spatial derivative of displacement $u$.

In contrast, under the framework of the DPL model, the relation between the heat flux and the temperature gradient is far more complicated (see Eq. (3)). As Al-Nimr states in [23], there is no guarantee that the heat flux and the temperature gradient would assume opposite signs under the effect of the DPL model, sharply contrary to the prediction of the classical diffusion theory. Therefore the "chain-link" between the sign of the heat flux and the direction of heat transfer is not valid anymore. In fact, the energy might even transfer in the direction of increasing temperature, whose entropy production can only be described by the non-equilibrium formula [23] so as to comply with the second law of thermodynamics. As a result, one simply cannot determine the direction of heat flow based on the polarity of the heat flux.

Nevertheless, from the cognitive information gathered in Figs. 5–8, a plainly qualitative relation between the temperature, the heat flux and the direction of heat transfer in this example can be briefly deduced a posteriori. By comparison, it seems that the heat flux positivity firmly depends on the direction of energy transportation and the sign of thermal wave temperatures. Assuming the direction along the $\xi$-axis to be positive (i.e., from left to right), it is concluded that, regardless of $Z_T$, positive heat flux corresponds to the combination of being both positive in temperature and direction of propagation or neither (see Figs. 5 and 7), while negative heat flux only manifests itself if either temperature or direction of energy propagation turns negative (see Figs. 6 and 8).

### 4.3. Thermal accumulation induced by $\tau_T$-related dispersion

Thermal concentration, i.e., the abrupt increase of temperature near the boundary due to the superposition of incident wave and reflective wave, is a phenomenon of enormous controversy surrounding the thermal wave model ($\tau_T = 0$) (Tzou [14] points out that the temperature overshooting due to the arrival of a thermal wave front results from mathematical idealization since the physical scale for this phenomenon to actually happen is beyond the continuum hypothesis. Nevertheless, he admits himself that it is consistent with the mathematical model of the classical thermal wave conduction). We now demonstrate that, in the framework of the DPL model, there exists a thermal accumulation phenomenon, which is associated with the phase lag of the temperature gradient $\tau_T$ and fundamentally different from thermal concentration in that it is dispersion-induced. To the authors' best knowledge, this phenomenon has not been reported in the literature.

Consider a semi-infinite region with an initial condition as defined in Eq. (13) and a periodic on–off thermal disturbance imposed on the surface

$$Q = \begin{cases} 2 & (n-1)P < \beta < (n-0.5)P \\ & \text{at } \xi = 0 \\ 0 & (n-0.5)P < \beta < nP \quad n = 1, 2, 3 \ldots \end{cases} \tag{25}$$

$$U = 0 \quad \xi \to \infty \tag{26}$$

with $n$ representing the number of period. We choose the duration of each period $P$ to be 0.1.

Fig. 10 shows the temperature distributions for $Z_q = 1$ and various $Z_T$ values. When $Z_T = 0$, distinct characteristics of thermal wave are preserved as ten thermal pulses propagate into the region from the left boundary (see Fig. 10a). As $Z_T$ increases, the initial shapes of thermal pulses are gradually deformed (see Fig. 10b–d). The phase lag of the temperature gradient $\tau_T$ causes strong attenuation to the sharp wave fronts through conduction. In addition, the locations of the temperature peaks (local temperature maxima) remain the same regardless of the value of $Z_T$, which implies the general speed of thermal wave propagation is independent of $\tau_T$.

It needs to be reiterated that technically the thermal signal at this moment travels at an infinite velocity. As noted before, the DPL heat conduction with non-zero $\tau_T$ is effectively parabolic such that any thermal disturbances is immediately felt everywhere in the medium. Yet strong wave features are still visible when $\tau_T < \tau_q$, which can be clearly seen in the previous section (Figs. 5–8). To understand this conceptual conflict, it is assumed that there coexist simultaneously two different processes in the DPL heat conduction [22,29]: Fourier-type fast process and Cattaneo-type slow process. The Cattaneo-type process,

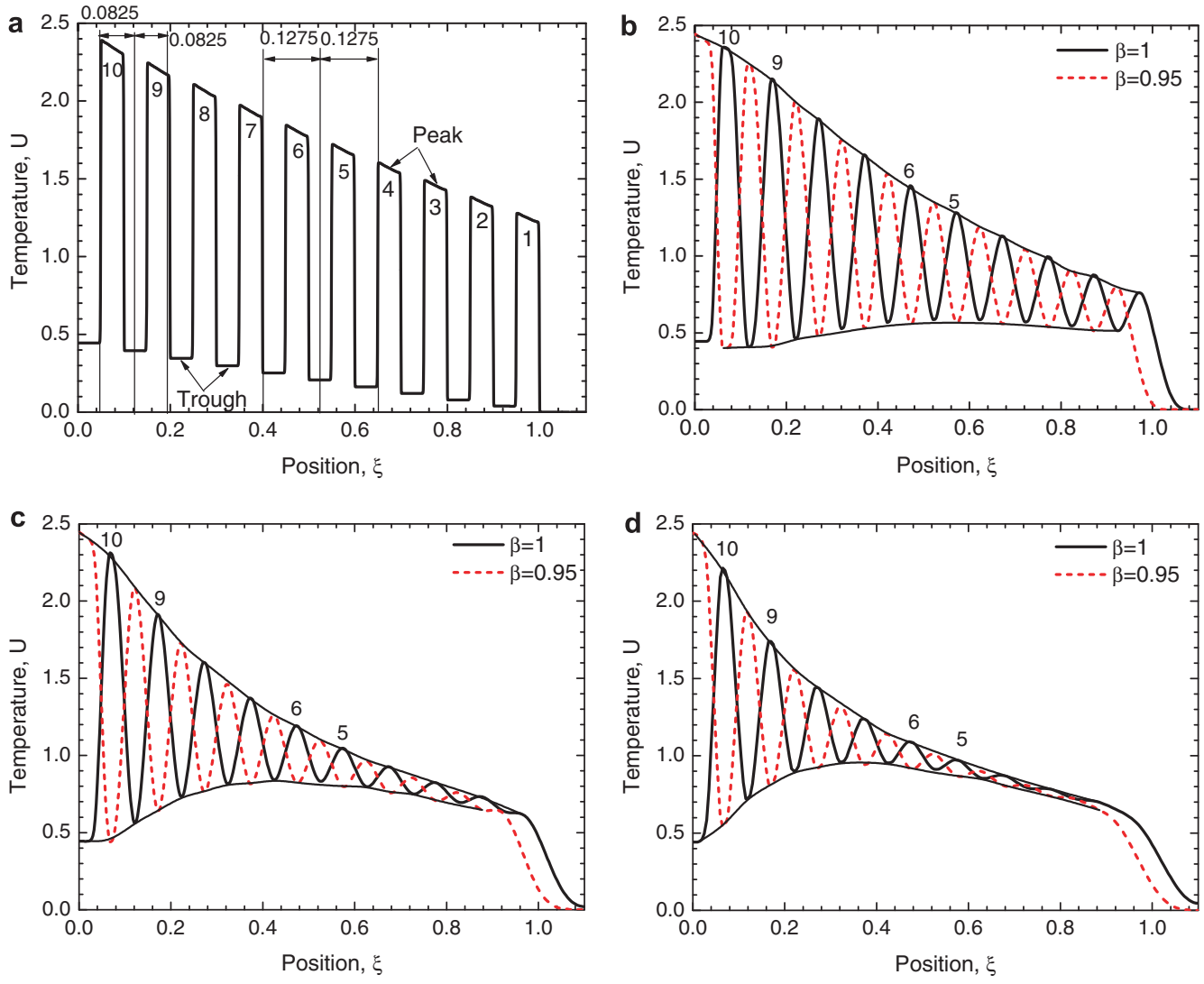


Fig. 10. Spatial temperature distributions in a semi-infinite region with initial condition defined in Eq. (13) and boundary conditions defined in Eqs. (25) and (26) for $Z_q = 1$ and (a) $Z_T = 0$; (b) $Z_T = 0.001$; (c) $Z_T = 0.002$; (d) $Z_T = 0.003$. The thin solid lines in Fig. 10 (b–d) are visual guide.

associated with $\tau_q$, corresponds to the classical thermal wave propagation and represents the wave feature in the DPL diffusion. The term "thermal wave propagation velocity" in our investigation, such as the speed of the temperature peaks mentioned above, is strictly related to this process. On the other hand, the Fourier-type process, associated with $\tau_T$, introduces an extra diffusive effect to the DPL heat conduction, which explains the attenuation of the wave front and the infinite speed of thermal disturbances.

In addition, it can be shown in Fig. 10, the amplitude of the temperature peaks stays declining along the direction of the thermal wave propagation with ever-increasing steepness as $Z_T$ increases. It is interesting to note, though, that the amplitude of the temperature troughs (local temperature minima) rise and fall over space under the effect of $Z_T$. Namely, the temperature troughs situated in the middle of the thermal-pulse succession, such as the one between thermal pulses No. 5 and No. 6, are noticeably higher than those near the two ends, such as the one between thermal pulses No. 9 and No. 10, as shown in Fig. 10b–d. At first glance, it seems paradoxical that the local temperature minima do not assume a monotonic distribution in space as the local temperature maxima do. In order to reach a better understanding of this phenomenon, we need to investigate the effect of $Z_T$ on the heat conduction of a single thermal pulse. Fig. 11 displays the separate propagation of thermal pulse No. 1 in the medium without any ensuing thermal pulses. A strong wave dispersion brought about by $Z_T$ can be seen in the temperature distributions: When $Z_T = 0$, the thermal wave pattern initially created is simply translated with damping amplitude as time elapses. The wave propagation shows of no sign of dispersion. However, with the increase of $Z_T$, the initial pulse is gradually deformed as it propagates. The width of the thermal pulse is considerably expanded, and it elevates the temperature where it would have maintained undisturbed otherwise, causing a larger heat-affected zone. In spite of the fact that the wave peak travels at a constant

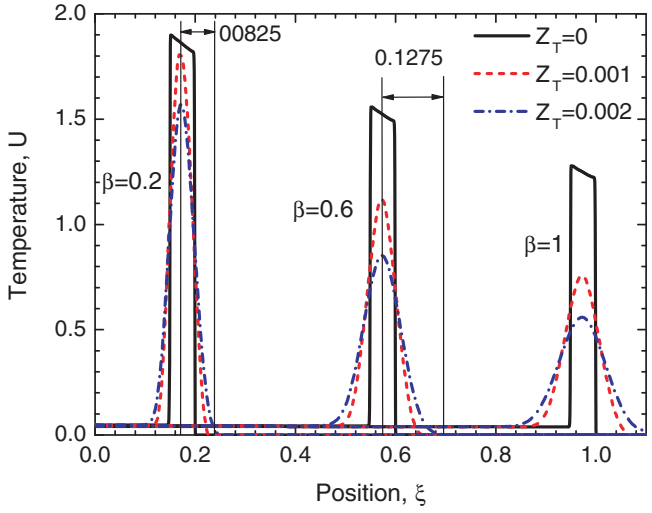


Fig. 11. Spatial temperature distributions for thermal pulse No. 1 propagating in the medium.

velocity determined by $Z_q$, the portion of the pulse in front of the peak must propagate at a faster velocity while the portion behind it must propagate at a slower velocity under the effect of $Z_T$. Spreading of propagation velocity is typical of wave dispersion.

Therefore, with the on–off type heat flux boundary, increasing pulse width for non-zero $Z_T$ results in the temperature at an arbitrary point not only being influenced by the most adjacent thermal pulses, but by those in whose out-stretched heat-affected zone this point resides as well. This extra temperature "gain" caused by the diffusive effect of $\tau_T$ can be dominant where the temperature predicted under the thermal wave model ($\tau_T = 0$) is relatively low, such as at the temperature troughs. Taking advantage of their locations, the temperature troughs in the middle may obtain more of this "extra" temperature increment than those near the both ends. For example, as shown in Fig. 11, the heat-affected radius of a single thermal pulse near the boundary is approximately 0.0825 when $Z_T = 0.002$. As a result, the local temperature minimum next to the boundary can only be influenced by those thermal pulses that roughly fall into the radius of 0.0825 centered at that point for the same $Z_T$, i.e., thermal pulses No. 9 and No. 10 (see Fig. 10a). In contrast, as shown in Fig. 11, the heat-affected radius for $Z_T = 0.002$ grows to 0.1275 when the thermal pulse propagate to $\xi = 0.6$. This implies that other than thermal pulses No. 5 and No. 6, both thermal pulses No. 4 and No. 7 can most certainly contribute to the increase of the amplitude of the temperature trough between thermal pulses No. 5 and No. 6 (see Fig. 10a). It is worth mentioning though, despite the fact that the heat-affected radius continues to grow when the thermal pulse reaches $\xi = 1.0$ as shown in Fig. 11, the value of temperature trough between thermal pulses No. 1 and No. 2 fails to top that between pulses No. 5 and No. 6 (see Figs. 10b–d). It is mainly because of the pre-existing spatial distribution of the declining temperature troughs along the direction of thermal propagation without the influence of $Z_T$ as shown in Fig. 10a, which also explains why the largest temperature trough is not located right at the midpoint of the succession of thermal pulses (see Figs. 10b–d), but slightly on the left side of it instead. Consequently, the local temperature minima in the middle exceed those at both ends, and even more so as $Z_T$ increases, as shown in Fig. 10b–d.

From the standpoint of energy transportation, $\tau_T$-related wave dispersion prescribes that energy should transfer at different velocities. That is to say, the portion that precedes the pulse peak propagates apparently faster than the portion behind. (Note that, in this fashion, the assumption of infinite velocity of thermal disturbances in the framework of the DPL model with non-zero $\tau_T$ can be perfectly satisfied at an infinitely distant point.) As a direct result of the difference in propagating velocity, a certain amount of energy is more likely to be trapped in the middle of a succession of thermal pulses (see Fig. 10b–d), causing severe thermal accumulation.

### 4.4. Moving-medium paradox

Galilean invariance states that fundamental laws of physics are the same in all inertial frames of reference. This principle is a basic requirement for any physical model, yet often overlooked in occasions that involve alternative or unconventional interpretations to various phenomena in continuous matter. In hydrodynamic simulation, Galilean invariance has become one of the major standards any innovative lattice-based hydrodynamics model needs to comply with before being considered "safe" to apply [30]. Likewise, in exploring the pseudo-particle behavior of the localized surface waves, lack of Galilean invariance could be a serious issue as well. For instance, Boussinesq's original model for weakly nonlinear long waves was proved to be problematic as his approximation fails to satisfy Galilean invariance in the moving frame [31].

As for non-Fourier heat conduction, Christov and Jordan [32] stated that if a moving continuum is considered, the usual form of the thermal wave equation leads to a paradoxical result that ultimately violates Galileo's principle of relativity. As a newly-developed macroscopic model designed to incorporate microscopic collision-based effects (two-step electron–phonon interaction [12], phonon-scattering [13]) in thermal process, the DPL model, in a strong likelihood, could be susceptible to such theoretical deficiency as well. We hereinafter demonstrate that, if a body is in motion, the local time derivatives in the DPL equation must be replaced by the material derivatives so as to guarantee Galilean invariance.

In convective heat transfer, the mass conservation principle should be taken into consideration

$$\frac{\mathrm{D}\rho}{\mathrm{D}t} + \rho\nabla\cdot\mathbf{u} = 0 \tag{27}$$

where

$$\frac{\mathrm{D}}{\mathrm{D}t} \overset{\text{def}}{=} \frac{\partial}{\partial t} + \mathbf{u}\cdot\nabla \tag{28}$$

represents the material derivative operator which is frequently encountered in convective heat and mass transfer. The energy equation neglecting viscous dissipation, internal heat generation and compressibility effect is given as

$$\rho c_p \frac{\mathrm{D}T}{\mathrm{D}t} + \nabla\cdot\mathbf{q} = 0 \tag{29}$$

For convenience of analysis, we consider a one-dimensional medium with constant thermal properties that moves at a constant velocity u. Directly substituting the DPL constitutive equation with local partial time derivatives (Eq. (6)) into the convective energy conservation equation yields

$$\frac{\partial T}{\partial t} + u\frac{\partial T}{\partial x} + \tau_q\left(\frac{\partial^2 T}{\partial t^2} + u\frac{\partial^2 T}{\partial t\partial x}\right) = \alpha\left(\frac{\partial^2 T}{\partial x^2} + \tau_T\frac{\partial^3 T}{\partial t\partial x^2}\right) \tag{30}$$

With the same dimensionless parameters defined in Eqs. (8a)–(8f) and an additional dimensionless velocity given as

$$\Lambda = \frac{uL}{\alpha} \tag{31}$$

the dimensionless form of Eq. (30) is formulated as

$$\frac{\partial U}{\partial\beta} + \Lambda\frac{\partial U}{\partial\xi} + Z_q\frac{\partial^2 U}{\partial\beta^2} + Z_q\Lambda\frac{\partial^2 U}{\partial\beta\partial\xi} = \frac{\partial^2 U}{\partial\xi^2} + Z_T\frac{\partial^3 U}{\partial\beta\partial\xi^2} \tag{32}$$

When $\Lambda = 0$, Eq. (32) reduces to the DPL heat conduction equation in the resting medium. Now combining the above governing equation with the initial-boundary conditions given in Eqs. (13)–(15)—except that the boundary conditions are set to be moving with the medium at the same velocity, i.e., imposed on the moving plane $\xi = \Lambda\beta$—constitutes a closed initial-boundary value problem. Note that the heat in the medium always transfers in the positive direction, from the left end to the right end, to be specific, whereas the medium itself could move in both directions in regard to the polarity of $\Lambda$. According to Galilean relativity, the laws of physics shall remain invariant for every observer moving parallel with a constant speed along a straight line, which implies that, in a reference frame which is attached to the moving medium, the heat conduction process should be exactly the same as in the resting body. (For instance, heating a pot of coffee takes the same period of time whether it is in your kitchen or on a maglev train that travels at 500 km/h).

As an indication whether or not the DPL model complies with Galilean invariance, we conduct the Galilean transformations to Eq. (32), following Christov and Jordan's example [32]. In detail, the coordinate system is changed from the resting frame to a kinetic frame moving with the medium.

$$\chi = \xi - \Lambda\beta \tag{33}$$

$$\beta = \beta \tag{34}$$

$$\theta(\chi,\beta) = U(\xi,\beta) \tag{35}$$

$$\Psi(\chi,\beta) = Q(\xi,\beta) \tag{36}$$

Hence, the mathematical statement of the DPL heat conduction problem in the moving frame yields

$$\frac{\partial\theta}{\partial\beta} + Z_q\frac{\partial^2\theta}{\partial\beta^2} - Z_q\Lambda\frac{\partial^2\theta}{\partial\beta\partial\chi} = \frac{\partial^2\theta}{\partial\chi^2} + Z_T\left(\frac{\partial^3\theta}{\partial\beta^2\partial\chi} - 2\Lambda\frac{\partial^3\theta}{\partial\beta\partial\chi^2} + \Lambda^2\frac{\partial^3\theta}{\partial\chi^3}\right) \tag{37}$$

The initial and boundary conditions of the problem in discussion are reformulated as

$$\theta = 0 \quad \text{and} \quad \frac{\partial\theta}{\partial\beta} = 0 \quad \text{at } \beta = 0 \tag{38}$$

$$\theta = 1 \quad \text{at } \chi = 0 \tag{39}$$

$$\Psi = 0 \quad \text{at } \chi = 1 \tag{40}$$

Compared with the governing equation in the resting body

$$\frac{\partial U}{\partial\beta} + Z_q\frac{\partial^2 U}{\partial\beta^2} = \frac{\partial^2 U}{\partial\xi^2} + Z_T\frac{\partial^3 U}{\partial\beta\partial\xi^2} \tag{41}$$

it is obvious that Eqs. (37) and (41) do not share the same mathematical appearance, nor can Eq. (37) be converted to Eq. (41) in any way. In Fig. 12, the spatial temperature distributions corresponding to Eq. (37) at the instant $\beta = 0.5$ for different $\Lambda$'s are obtained by employing the same TVD scheme with renewed variables

$$\begin{bmatrix} W_1 \\ W_2 \end{bmatrix} = \begin{bmatrix} \frac{\Psi}{\sqrt{\Lambda^2+\frac{4}{Z_q}}} + \left(\frac{1}{2} + \frac{1}{2}\frac{\Lambda}{\sqrt{\Lambda^2+\frac{4}{Z_q}}}\right)\theta \\ -\frac{\Psi}{\sqrt{\Lambda^2+\frac{4}{Z_q}}} + \left(\frac{1}{2} - \frac{1}{2}\frac{\Lambda}{\sqrt{\Lambda^2+\frac{4}{Z_q}}}\right)\theta \end{bmatrix} \tag{42}$$

$$\begin{bmatrix} \lambda_1 \\ \lambda_2 \end{bmatrix} = \begin{bmatrix} -\frac{1}{2}\Lambda + \frac{1}{2}\sqrt{\Lambda^2+\frac{4}{Z_q}} \\ -\frac{1}{2}\Lambda - \frac{1}{2}\sqrt{\Lambda^2+\frac{4}{Z_q}} \end{bmatrix} \tag{43}$$

$$\begin{bmatrix} G_1 \\ G_2 \end{bmatrix} = \begin{bmatrix} -\frac{\Psi}{Z_q\sqrt{\Lambda^2+\frac{4}{Z_q}}} - \frac{D}{Z_q\sqrt{\Lambda^2+\frac{4}{Z_q}}} \\ \frac{\Psi}{Z_q\sqrt{\Lambda^2+\frac{4}{Z_q}}} + \frac{D}{Z_q\sqrt{\Lambda^2+\frac{4}{Z_q}}} \end{bmatrix} \tag{44}$$

where

$$D = Z_T\left(\frac{\partial^2\theta}{\partial\chi\partial\beta} - \Lambda\frac{\partial^2\theta}{\partial\chi^2}\right) \tag{45}$$

As Fig. 12 shows, the propagation of the thermal wave actually depends on $\Lambda$ in the moving frame attached to the medium in motion under different $Z_T$ values, which is obviously unphysical. There exists clear phase shifts in connection with $\Lambda$ in the spatial temperature distributions: The temperature curves with positive $\Lambda$ values lags behind the reference curves with zero $\Lambda$, while the ones with negative

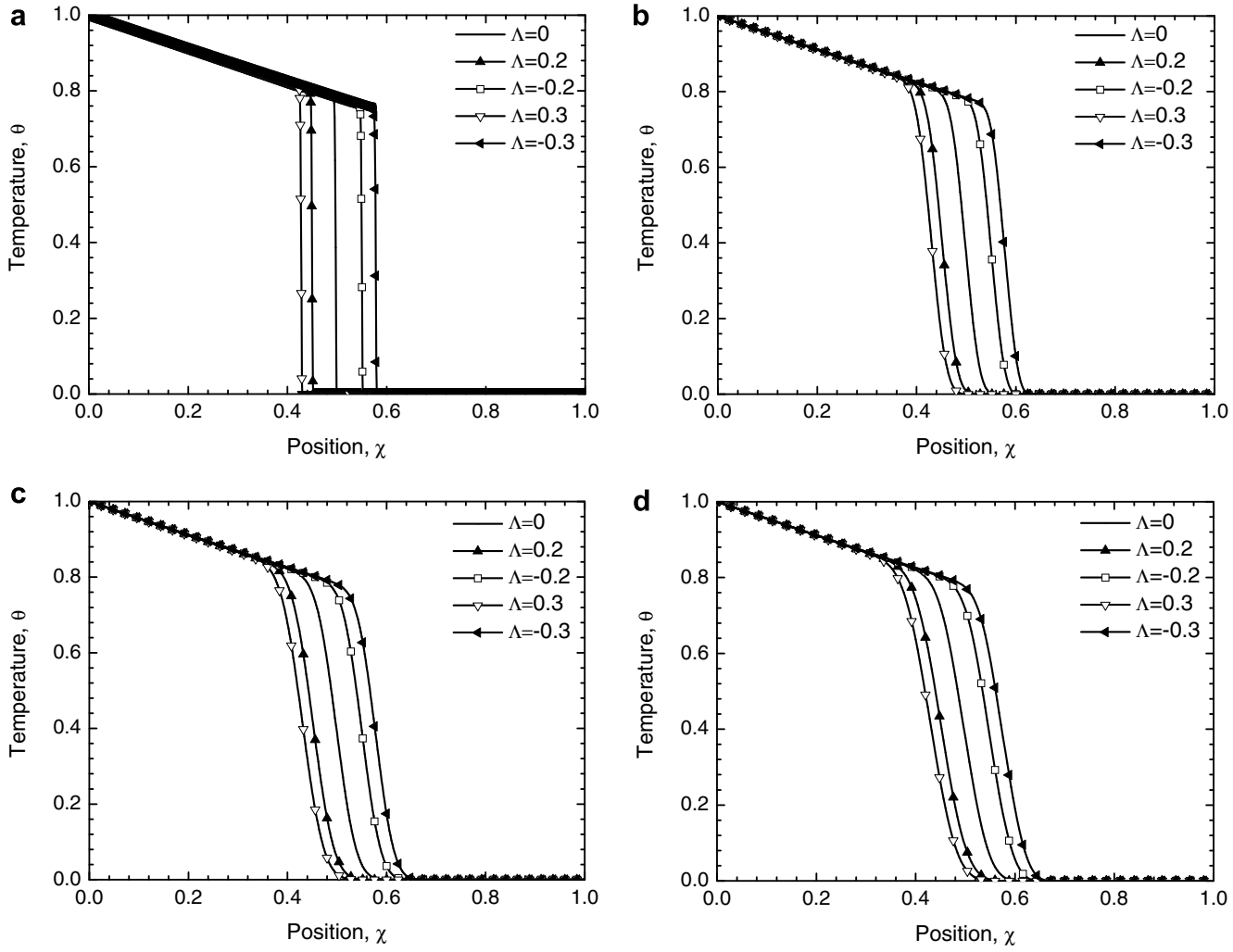


Fig. 12. Spatial temperature distributions for the heat conduction problem defined in Eq. (37)–(41) in the moving frame at $\beta = 0.5$ for various $\Lambda$ values, $Z_q = 1$ and (a) $Z_T = 0$; (b) $Z_T = 0.001$; (c) $Z_T = 0.002$; (d) $Z_T = 0.003$.

$\Lambda$ values precedes the reference curves. It is also found that the phase differences are the sole product of $\Lambda$, with increasing $\Lambda$ predicting larger phase differences. Namely, no connection is detected between phase differences and $Z_T$ (see Fig. 12a–d). Such singularity indicates that, in the moving body, the generalized thermal waves transmit apparently faster if the heat transports in the opposite direction of the moving medium ($\Lambda < 0$), whereas in contrast they appear to be slower if the heat and the medium in which the conduction process occurs happen to move in the same direction ($\Lambda > 0$). The above findings are clearly at odds with Galileo's principle of relativity. Therefore, it is pretty obvious that directly applying the DPL heat conduction model in convective heat transfer may lead to erroneous results. It is worth noting that, only the results for $Z_T < Z_q$ are available in Fig. 12 because no discernible pattern, such as the clear and simple phase shift, can be recognized in association with the dimensionless velocity $\Lambda$ for the case of diffusion ($Z_T = Z_q$) or over-diffusion ($Z_T > Z_q$). Strong high-order effect attributed to large $Z_T$ values (see Eq. (37)) brings drastic variations onto the temperature distribution curves in the presence of even small fluctuation of $\Lambda$, which is beyond the scope of the paper.

So as to alleviate this physical defect, we replace the partial time-derivatives in the Taylor expansion form of the DPL model with the material derivatives defined in Eq. (28) in a similar way that Christov and Jordan [32] treated the thermal wave model. The modified DPL model in a moving medium is thus given as

$$\left[1 + \tau_q\left(\frac{\partial}{\partial t} + \mathbf{u}\cdot\nabla\right)\right]\mathbf{q} = -k\left[1 + \tau_T\left(\frac{\partial}{\partial t} + \mathbf{u}\cdot\nabla\right)\right]\nabla T \tag{46}$$

Combining Eq. (46) and the one-dimensional energy conservation equation with the same assumptions we have made so far (no viscous dissipation, internal heat generation or compressibility effect, along with constant thermal properties and constant moving velocity), then repeating the previous operation of non-dimensionalization leads to

$$\frac{\partial U}{\partial \beta}+\Lambda\frac{\partial U}{\partial \xi}+Z_q\frac{\partial^2 U}{\partial \beta^2}+2Z_q\Lambda\frac{\partial^2 U}{\partial \beta\partial \xi}+Z_q\Lambda^2\frac{\partial^2 U}{\partial \xi^2}=\frac{\partial^2 U}{\partial \xi^2}+Z_T\frac{\partial^3 U}{\partial \beta\partial \xi^2}+Z_T\Lambda\frac{\partial^3 U}{\partial \xi^3} \tag{47}$$

Under the Galilean transformations defined in Eqs. (33)–(36), the above rather complicated equation can be reduced to a surprisingly simple form

$$\frac{\partial \theta}{\partial \beta}+Z_q\frac{\partial^2 \theta}{\partial \beta^2}=\frac{\partial^2 \theta}{\partial \chi^2}+Z_T\frac{\partial^3 \theta}{\partial \beta\partial \chi^2} \tag{48}$$

which also coincides with Eq. (41), the heat conduction equation in the resting body. The effect of $\Lambda$ is completely eliminated from the heat transfer process in the kinetic frame moving with the medium, which provides evidence more than enough that the modified form of the DPL model is strictly Galilean invariant.

In general three-dimensional form, the modified DPL model in the material framework (Eq. (46)), along with the mass conservation equation (Eq. (27)) and the energy conservation equation (Eq. (29)) constitutes a group of governing equations for non-Fourier convective heat transfer (with velocity field assumed known)

$$\begin{cases}\frac{\partial \rho}{\partial t}+\nabla\cdot(\rho\mathbf{u})=0\\ \left[1+\tau_q\left(\frac{\partial}{\partial t}+\mathbf{u}\cdot\nabla\right)\right]\mathbf{q}=-k\left[1+\tau_T\left(\frac{\partial}{\partial t}+\mathbf{u}\cdot\nabla\right)\right]\nabla T\\ \rho c_p\left(\frac{\partial}{\partial t}+\mathbf{u}\cdot\nabla\right)T+\nabla\cdot\mathbf{q}=0\end{cases} \tag{49}$$

In a frame moving with constant velocity $\mathbf{V}$ ($\mathbf{V}$ and $\mathbf{u}$ could be different), we have

$$\boldsymbol{\chi}=\mathbf{r}-\mathbf{V}t \tag{50}$$

$$t=t \tag{51}$$

$$\Omega(\boldsymbol{\chi},t)=T(\mathbf{r},t) \tag{52}$$

$$\boldsymbol{\Psi}(\boldsymbol{\chi},t)=\mathbf{q}(\mathbf{r},t) \tag{53}$$

$$\mathbf{v}(\boldsymbol{\chi},t)=\mathbf{u}-\mathbf{V} \tag{54}$$

$$P(\boldsymbol{\chi},t)=\rho(\mathbf{r},t) \tag{55}$$

where $\mathbf{v}$ denotes the relative velocity of the moving frame to the medium in motion. By introducing these variables into Eq. (49), the governing equations of the heat convection process under the modified DPL model in the moving frame is hence derived as

$$\begin{cases}\frac{\partial P}{\partial t}+\nabla\cdot(P\mathbf{v})=0\\ \left[1+\tau_q\left(\frac{\partial}{\partial t}+\mathbf{v}\cdot\nabla\right)\right]\boldsymbol{\Psi}=-k\left[1+\tau_T\left(\frac{\partial}{\partial t}+\mathbf{v}\cdot\nabla\right)\right]\nabla\Omega\\ Pc_p\left(\frac{\partial}{\partial t}+\mathbf{v}\cdot\nabla\right)\Omega+\nabla\cdot\boldsymbol{\Psi}=0\end{cases} \tag{56}$$

which once again takes the same form as Eq. (49). We are thus assured that the modified DPL model (with the partial temporal derivatives replaced by the material derivatives) complies with Galileo's principle of relativity. That is, generally speaking, the mechanism of energy transportation process in a moving medium remains unchanged in any inertial frame of reference. Such governing equations (Eq. (49)) could be of tremendous practical worth in describing the heat transfer process in forced flow of superfluid helium, where non-Fourier thermal behaviors (including thermal wave and diffusion-like [2] mechanism) have to be dealt with properly.

## 5. Conclusions

A number of interesting non-Fourier thermal behavior under the dual-phase-lag model in response to various initial and boundary conditions are investigated numerically in this study. The analytical process employs a high-order explicit TVD scheme based on characteristics. A number of irregularities in the heat conduction are detected and analyzed. The following conclusions are drawn:

1. Under the mode of over-diffusion ($\tau_q<\tau_T$), the DPL model predicts a "hyper-active" to "under-active" thermal behavior due to the fact that $\tau_T$ exerts different effects on the heat conduction throughout the transient process. The diffusion-like behavior related to $\tau_T$ acts as a promoting force at the early stage of heat conduction after the initial thermal balance is broken ascribed to the surface thermal disturbance, and then gets more and more impeding as new equilibrium is being established.
2. For $\tau_q>\tau_T$ (when wave nature in the heat conduction is still observable), negative-temperature thermal wave reflection can be obtained if boundary temperature is hold constant. This phenomenon is analogous to the polarity change of displacement for reflected mechanical waves at a fixed-end boundary. Its direct implication states that heating process may turn into cooling effect in the framework of the DPL model. On the other hand, reflected thermal waves assume negative heat fluxes if adiabatic boundary condition is present, which is similar to the polarity change of stress for reflected mechanical waves at a free-end boundary.
3. A localized thermal accumulation that is closely related with $\tau_T$ is detected during an on–off periodic heating process, which differs from the well-known thermal concentration effect that the thermal wave model predicts. The underlying cause for the former phenomenon is associated with the dispersive effect that $\tau_T$ brings into the thermal wave propagation, whereas the latter is the product of wave superposition.
4. Direct application of the DPL model into the convective heat transfer may lead to physically unrealistic results that explicitly violate Galilean invariance. A modified version of the DPL model with the material derivatives is proposed to describe the relations between the heat flux and the temperature gradient if the medium is in motion. Such description may be of benefit in solving practical problems, such as forced flow of superfluid helium.

The dual-phase-lag model, as a general solution aiming at covering various thermal behaviors ranging from micro-

to macro-scale heat transfer, shows great promise and potential for offering a unified approach to heat transport problem in day-to-day engineering practice. The physical anomalies that we presented in detail in this paper are meant to provide us better insights into the unique and exciting physical properties the DPL model possesses, the experimental validation of which, however, should be the focus of our future research.

## Acknowledgement

This research is jointly supported by A Foundation for the Author of National Excellent Doctoral Dissertation of PR China (200236) and NCET.

## References

[1] D.E. Glass, M.N. Özişik, Brian Vick, Non-Fourier effects on transient temperature resulting from periodic on–off heat flux, Int. J. Heat Mass Transfer 30 (1987) 1623–1630.
[2] P. Zhang, M. Murakami, R.Z. Wang, Study of the transient thermal wave heat transfer in a channel immersed in a bath of superfluid helium, Int. J. Heat Mass Transfer 49 (2006) 1384–1394.
[3] C. Cattaneo, Sur une forme de l'équation de la chaleur éliminant le paradoxe d'une propagation instantanée, Comptes Rendus 247 (1958) 431–433.
[4] P. Vernotte, Les paradoxes de la théorie continue de l'équation de la chaleur, Comptes Rendus 246 (1958) 3154–3155.
[5] D.W. Tang, N. Araki, Non-Fourier heat conduction in a finite medium under periodic surface thermal disturbance, Int. J. Heat Mass Transfer 39 (1996) 1585–1590.
[6] Kuo-Chi Liu, Han-Taw Chen, Numerical analysis for the hyperbolic heat conduction problem under a pulsed surface disturbance, Appl. Math. Comput. 159 (2004) 887–901.
[7] D.E. Glass, M.N. Özişik, D.S. McRae, Hyperbolic heat conduction with temperature-dependent thermal conductivity, J. Appl. Phys. 59 (1986) 1861–1865.
[8] Vladimir V. Kulish, Vasily B. Novozhilov, The relationship between the local temperature and the local heat flux within a one-dimensional semi-infinite domain of heat wave propagation, Math. Probl. Eng. 4 (2003) 173–179.
[9] D.W. Tang, N. Araki, Non-Fourier heat conduction in a finite medium under periodic surface thermal disturbance—II. Another form of solution, Int. J. Heat Mass Transfer 39 (1996) 3305–3308.
[10] H. Herwig, K. Becket, Fourier versus non-Fourier heat conduction in materials with a nonhomogeneous inner structure, J. Heat Transfer 122 (2000) 363–365.
[11] C. Körner, H.W. Bergmann, The physical defects of the hyperbolic heat conduction equation, Appl. Phys. A 67 (1998) 397–401.
[12] S.I. Anisimov, B.L. Kapeliovich, T.L. Perel'man, Electron emission from metal surfaces exposed to ultra-short laser pulses, Soviet Phys. JETP 39 (1974) 375–377.
[13] R.A. Guyer, J.A. Krumhansl, Solution of the linearized phonon Boltzmann equation, Phys. Rev. 148 (1966) 766–780.
[14] D.Y. Tzou, A unified field approach for heat conduction from marcro- to micro-scales, ASME J. Heat Transfer 117 (1995) 8–16.
[15] Paul J. Antaki, New interpretation of non-Fourier heat conduction in processed meat, ASME J. Heat Transfer 127 (2005) 189–193.
[16] D.Y. Tzou, K.S. Chiu, Temperature-dependent thermal lagging in ultrafast laser heating, Int. J. Heat Mass Transfer 44 (2001) 1725–1734.
[17] Kuo-Chi Liu, Analysis of dual-phase-lag thermal behavior in layered films with temperature-dependent interface thermal resistance, J. Phys. D: Appl. Phys. 38 (2005) 3722–3732.
[18] D.Y. Tzou, M.N. Özişik, R.J. Chiffelle, The lattice temperature in the microscopic two-step model, ASME J. Heat Transfer 116 (1994) 1034–1038.
[19] Paul J. Antaki, Solution for non-Fourier dual phase lag heat conduction in a semi-infinite slab with surface heat flux, Int. J. Heat Mass Transfer 41 (1998) 2253–2258.
[20] D.W. Tang, N. Araki, Wavy, wavelike, diffusive thermal responses of finite rigid slabs to high-speed heating of laser-pulses, Int. J. Heat Mass Transfer 42 (1999) 855–860.
[21] H.Q. Yang, Characteristics-based, high-order accurate and nonoscillatory numerical method for hyperbolic heat conduction, Numer. Heat Transfer, Part B 18 (1990) 221–241.
[22] X.M. Zhou, K.K. Tamma, C.V.D.R. Anderson, On a new C- and F-processes heat conduction constitutive model and the associated generalized theory of thermoelasiticity, J. Thermal Stresses 24 (2001) 531–564.
[23] M.A. Al-Nimr, M. Naji, V.S. Arbaci, Nonequilibrium entropy production under the effect of the dual-phase-lag heat conduction model, ASME J. Heat Transfer 122 (2000) 217–223.
[24] D.Y. Tzou, Macro- to microscale heat transfer: the lagging behavior, Taylor & Francis, New York:, 1997, pp. 111-138.
[25] W. Shen, S. Han, A numerical solution of two-dimensional hyperbolic heat conduction with non-linear boundary conditions, Heat Mass Transfer 39 (2003) 499–507.
[26] Vladimir V. Kulish, Vasily B. Novozhilov, An integral equation for the dual-lag model of heat transfer, ASME J. Heat Transfer 126 (2004) 805–808.
[27] W.-B. Loi, H.-S. Chu, Effect of interface thermal resistance on heat transfer in a composite medium using the thermal wave model, Int. J. Heat Mass Transfer 43 (2000) 653–663.
[28] A. Hji-Sheikh, W.J. Minkowycz, E.M. Sparrow, Certain anomalies in the analysis of hyperbolic heat conduction, ASME J. Heat Transfer 124 (2002) 307–319.
[29] D.D. Joseph, L. Preziosi, Heat waves, Rev. Modern Phys. 61 (1) (1989) 41–73.
[30] P. Lallemand, L.–S. Luo, Theory of the lattice Boltzmann method: Dispersion, dissipation, isotropy, Galilean invariance, and stability, Phys. Rev. E 61 (6) (2000) 6546–6562.
[31] C.I. Christov, An energy-consistent dispersive shallow-water model, Wave Motion 34 (2001) 161–174.
[32] C.I. Christov, P.M. Jordan, Heat conduction paradox involving second-sound propagation in moving media, Phys. Rev. Lett. 94 (2005). Art. No. 154301.